Supplementary Materials

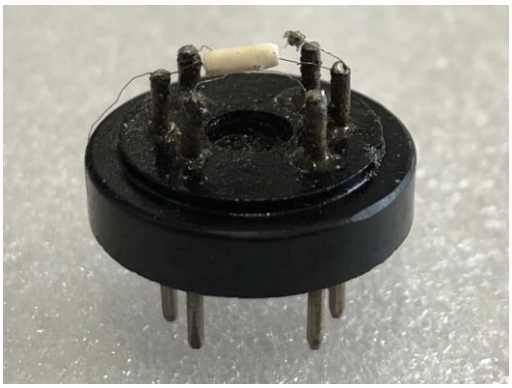

Figure S1: gas sensor used for characterizing gas sensing behavior of samples

Figure S1 showed the heater-type gas sensor. The gas sensing materials were pasted on surface of the Alumina tube containing gold electrodes. The Ni-Cr heating wires were inserted through the Alumina tube to regulate heating during gas sensing measurement.

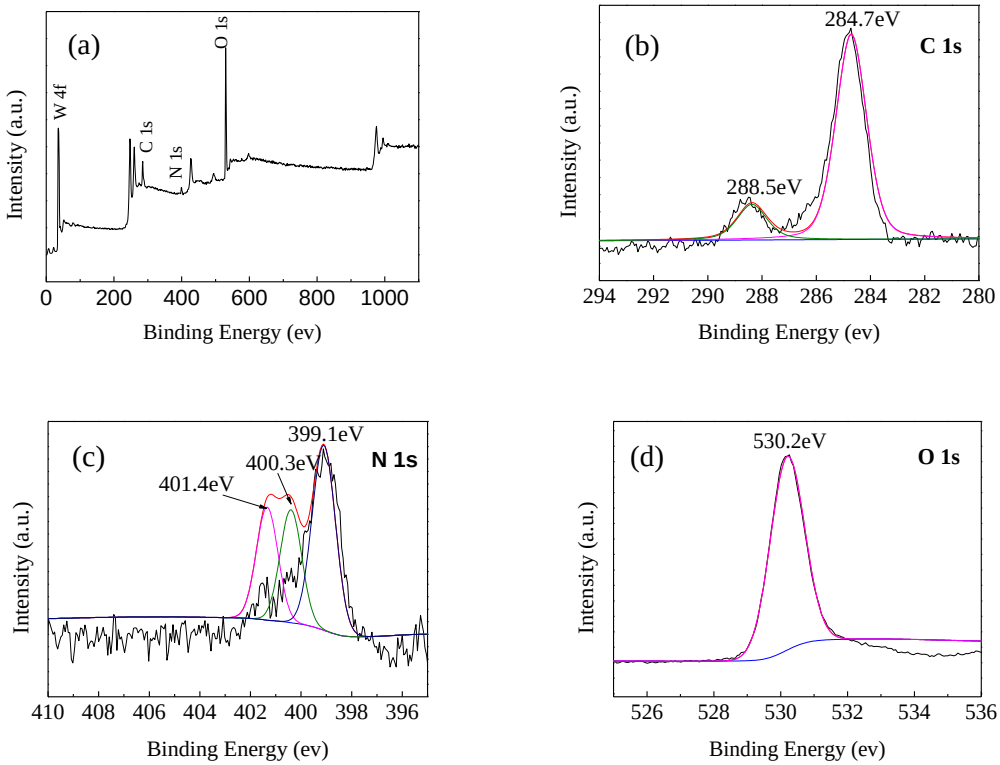

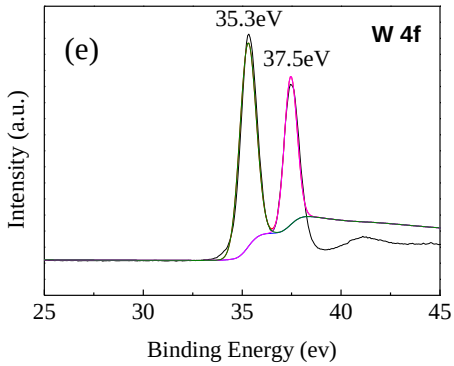

Figure S2: XPS spectra of g-C_3N_4-WO_3 (S-2): (a) full spectrum. (b) C1s. (c) N1s. (d) O1s. (e) W 4f.

The XPS spectra of g-C_3N_4-WO_3 (S-2) are shown in supplemental Figure S2. As illustrated in Figure S2(a), the g-C_3N_4-WO_3 composite was composed of C, N, O and W. For the sake of understanding the chemical states of elements, the peaks of elements were deconvoluted. As shown in Figure S2(b), the peak representing the sp^2 carbon atom bonded to three N atoms was observed at 284.7 eV, and the peak resulting from sp^2 atoms in the aromatic ring bonded to $–NH_2$ and –NH at 288.5 eV [15, 16]; As shown in Figure S2(c), three peaks centered at 399.1, 400.3 and 401.4 eV were obtained from deconvolution of the N1s spectrum; The peak at 399.1 eV originated from N atoms in the aromatic ring observed at the edges of the graphite planes [15]; the peak at 400.3 eV corresponded to N atoms bonded trigonally with sp^2 or sp^3 hybridized carbon atoms [15]; and the peak centered at 401.4 eV was caused by N atoms bonded to hydrogen atoms [14]. The peak of O1s in Figure S2(d) could be dissociated into a couple of peaks centered at 530.2 and 531.7 eV, which could be attributed to lattice oxygen in WO_3 and hydroxyl radicals [14, 30]. As shown in Figure S2(e), the peaks at 35.3 eV and 37.5 eV were consistent with the typical binding energies of W 4f7/2 and W 4f5/2 of W^{6+}, which proved the existence of W^{6+} in the composite [16].

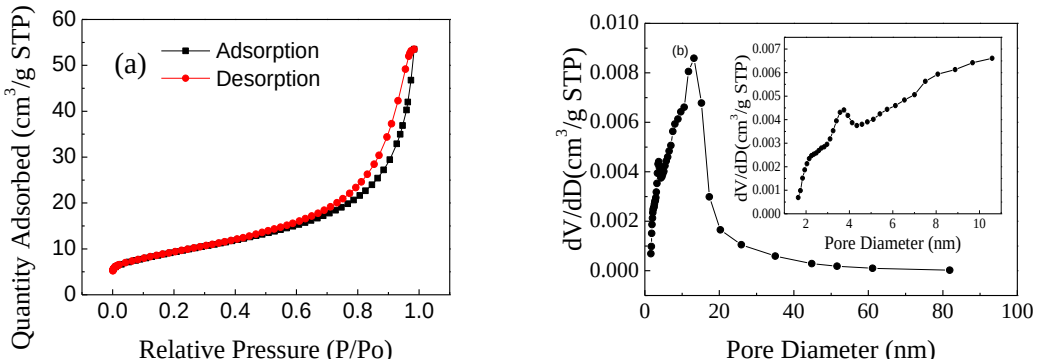

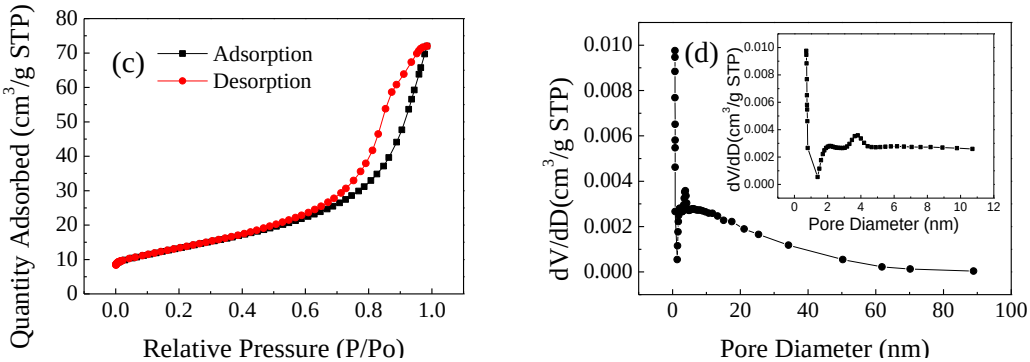

Figure S3: (a) N_2 adsorption-desorption isotherm of WO_3. (b) pore size distribution curve of WO_3. (c) N_2 adsorption-desorption isotherm of g-C_3N_4-WO_3 (S-2). (d) pore size distribution curve of g-C_3N_4-WO_3 (S-2).

The nitrogen adsorption and desorption isotherms of pure WO_3 and g-C_3N_4-WO_3 (S-2) are illustrated in supplemental Figure S3(a, c), the isotherms of both samples were classic type IV, which confirmed that mesopores existed in the two samples. Figure S3(b, d) shows the pore size distribution curves of pure WO_3 and g-C_3N_4-WO_3 (S-2), the average pore sizes were 9.4 and 9.9 nm, respectively; the samples had specific surface areas of 33.12 and 47.31 m^2/g, respectively, which indicated that the addition of g-C_3N_4 improved the specific surface area of g-C_3N_4-WO_3 composite; the increase of the specific surface area played a significant role in enhancement of gas sensing response.